Progress In Electromagnetics Research, Vol. 114, 481–493, 2011

EYE-SHAPED SEGMENTED READER ANTENNA FOR NEAR-FIELD UHF RFID APPLICATIONS

X. Li and J. Liao †

Key Laboratory of Universal Wireless Communications
Ministry of Education
Beijing University of Posts and Telecommunications
Beijing 100876, China

Y. Yuan and D. Yu

Radio access Technology and Solution (RTS) Corporate Technology
Siemens Ltd., China

Abstract—An eye-shaped segmented (ESS) antenna is presented for ultra-high frequency (UHF) near-field radio frequency identification (RFID) applications. The proposed antenna shows in-phase current even though the perimeter of the eye-shaped loop is comparable to the operating wavelength. The ESS antenna is fabricated on a FR4 printed circuit board (PCB) and embedded in a metal cavity with an overall size of $250 \times 180 \times 50\,\text{mm}^3$. The measured bandwidth is around 11 MHz (860–871 MHz) under the condition of VSWR less than 2.0, which covers the Europe standard (865 MHz–868 MHz) and agrees well with the simulated results. Finally, as a reader antenna in the RFID system, the measured read distance and read width can achieve 16.1 cm and 8 cm, respectively. The ESS antenna is desirable for UHF near-field RFID reader applications.

1. INTRODUCTION

Antennas, which directly affect the stability and reliability of the radio-frequency identification (RFID) system, receive a lot of attention. Usually, RFID can be used, for example, in identifying objects in warehousing, supply chain management, and other automation

Received 16 February 2011, Accepted 14 March 2011, Scheduled 15 March 2011
Corresponding author: Xiuping Li (xpli@bupt.edu.cn).
† X. Li and J. Liao are also with School of Electronic Engineering, Beijing University of Posts and Telecommunications, Beijing 100876, China.

processes. There are two kinds of RFID systems: near-field and far-field. Generally, the near-field RFID systems at low frequency (LF, 125–134 KHz) and high frequency (HF, 13.56 MHz) bands are based on inductive coupling to conduct power transfer and data transmission between the readers and the tags. The far-field RFID systems at ultra-high frequency (UHF, 840–960 MHz) and microwave (2.4 GHz and 5.8 GHz) bands use electromagnetic waves propagating between the readers and tags. In LF/HF RFID systems, the conventional solid line loop structure is used for both tag and reader antenna, since these electrically small loop antenna can produce strong and uniform magnetic field in the region near to the antenna. There is an optimal size for the best read distance for any given peak loop current and coupling requirement [1, 5]. The shortcoming of LF/HF RFID system is that it is hard to control the required read width and read range and the data transmission rate is lower compared to UHF systems. Due to the promising opportunities of item-level RFID applications in pharmaceutical and retailing industry [1–4], different kinds of UHF near-field antennas are investigated by researchers [5–7].

Compared to LF/HF near-field RFID systems, the coupling between the UHF near-field RFID reader antennas and the tags can be either magnetic (inductive) or electric (capacitive) with higher data transmission rate [1, 13]. Inductive coupling systems are preferred in most applications. Compared to radiatively coupled far-field UHF RFID system, the inductive coupling UHF near-field RFID system provides physically smaller tag and operates well in or close to aqueous fluids [5, 10–12, 14–17].

Two obstacles are encountered when one attempts to design simple loop antennas for UHF near-field readers. Firstly, when the loop perimeter is comparable to the wavelength at the operating frequency, the current distribution shifts to produce a change in sign of the current flow, and the antennas produce relatively little magnetic field on axis [5–7]. Secondly, the matching is needed since the antenna is awkward to match to 50 Ω input impedance.

In order to address the above two problems, a segmented loop antenna has been constructed [5–7]. In this paper, we propose an eye-shaped segmented (ESS) antenna, which can be tuned to control the read distance and read width. In this structure, the two neighbor parallel segments provide a series capacitance to the next segment. Each segment forms a resonant line, avoiding the accumulation of inductive reactance that otherwise impedes matching. The current around the loop also remains approximately in phase and of the same sign, thus producing a substantial magnetic field along the axis. The ESS antenna is fabricated and shows measured bandwidth around

11 MHz (860–871 MHz) under the condition of VSWR less than 2.0, which covers the Europe standard (865 MHz–868 MHz). Finally, by using the impinj UHF button near-field tag, read distance 16.1 cm and read width 8 cm are obtained in air, which matches well with simulated results by using Ansoft HFSS. In this paper, the reading distance shows 15/15.5 cm when the tag is attached to the water-containing items. Compared to far-field tags, where the reading distance will be decreased more than 60%, the reading distance of the near-field system is quite stable in or close to aqueous fluids environment.

The organization of the paper is as follows: the antenna structure and the current simulated results are introduced in Section 2. The antenna structure equivalent circuit model determination and its impedance measurement technique are described in Section 3. Based on Section 3, the antenna matching network is presented in Section 4. Section 5 shows the near and far-field performance and the comparison of measured and simulated read distance and read width, respectively. The conclusion is given in Section 6.

2. ANTENNA STRUCTURE AND DESIGN

Figure 1 shows a near-field UHF RFID system for item-level identification, where R presents the reader, d_1 presents the read distance, d_2 is the distance between the two items, and d_3 ($d_3 = d_2$) presents the read width. According to the industrial application specification, a reader antenna with read distance $d_1 \geq 15$ cm and read width $d_3 \leq 8$ cm are required.

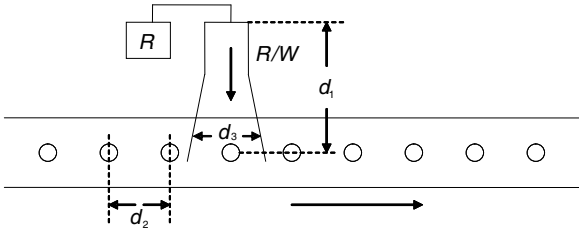

Figure 1. A Near-field UHF RFID system.

Commonly, a loop antenna with a length much smaller than its operating wavelength is referred to as a small loop. Small loops have constant current phase along the loop wire and have the capability of generating a strong near-field magnetic field. On the other hand, due to the small circumference, the magnetic field tapers off very quickly beyond a distance equivalent to one loop diameter. Increasing the

diameter of the loop increases the near-field read distance to some extent, however at UHF frequency, the loop is not small compared to the wavelength and the current along the loop will be out of phase.

The eye-shaped segmented loop is shown in Figure 2(a). A Cartesian coordinate system is oriented such that the upper surface of the FR4 PCB (thickness $h = 1.6\,\text{mm}$, relative dielectric constant $\varepsilon_r = 4.5$, and loss tangent $\tan\delta = 0.02$) in Figure 2 lies in the x-y plane. Figure 2(b) shows the 3-D view of the ESS antenna, which comprises ESS antenna, metal cavity and a lumped matching network. The ESS antenna and lumped matching network are symmetrically structured with respect to the centerline (y-axis).

In Figure 2(a), the capacitance C provided by the two neighbor parallel segments is decided by the electrical length θ and space d,

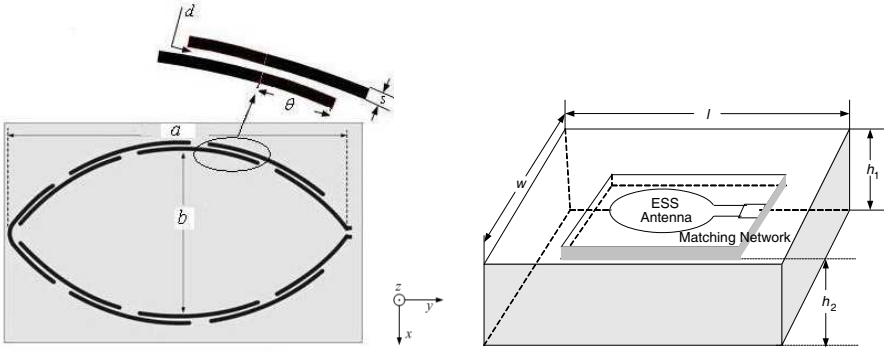

Figure 2. Eye-shaped segmented RFID reader antenna structure. (a) ESS antenna structure. (b) 3-D view structure.

Table 1. Dimensions of the proposed antenna.

Dimensions (mm)	a	160
	b	80
	l	250
	w	180
	h_1	50
	h_2	40
	d	1
	s	2
	θ	11.6

which can be expressed as follows:

$$C \propto \frac{\theta}{d} \tag{1}$$

Each segment is resonant with the capacitance, thus avoiding the current phase accumulation along the eye-shaped loop. By designing the length of the short and long axis, the read width and distance can be controlled less than 8 cm and larger than 15 cm, respectively.

In Figure 2(b), the metal cavity size is shown as $w \times l \times h_1$, and h_2 presents the distance of the antenna to the bottom of the cavity, where $h_1 - h_2 = 10$ mm. The antenna dimensions are shown in Table 1. The metal cavity has two functions: one is used to reduce the effect from outside of the antenna; another is to control the magnetic field in the required direction and increase the radiation efficiency. However, the metal cavity increases the antenna Q value, which increases the difficulty for broadband near-field antenna design.

The surface current along the eye-shaped loop without and with segmentation driven at 866 MHz is shown in Figures 3(a) and (b), respectively. Figure 3(a) shows current nulls and we can see that the top portion is out of phase with the bottom. The capacitance formed by two parallel segments combining the parasitic inductance of each section cause the large loop to behave electrically like a small one. The current remains constant along the segmented loop and provides a strong magnetic field as shown in Figure 3(b).

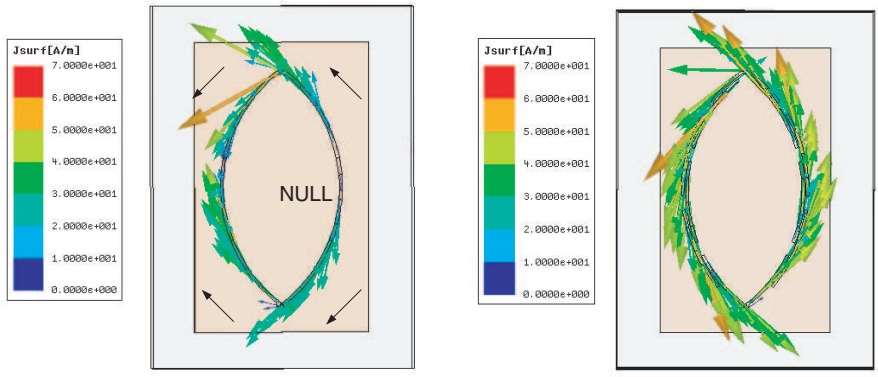

(a) (b)

Figure 3. Surface current distribution along the eye-shaped loop driven at 866 MHz. (a) Without segmentation. (b) With segmentation.

3. ANTENNA EQUIVALENT CIRCUIT MODEL AND ITS IMPEDANCE MEASUREMENT TECHNOLOGY

Figure 4 shows the equivalent circuit model of Figure 2(a), the initial value of the capacitance can be determined according to Equation (1), here $C = 0.95\,\text{pF}$.

Since

$$f = \frac{1}{2\pi\sqrt{L \cdot C}} \tag{2}$$

where $f = 866\,\text{MHz}$ is the center frequency. The initial value of the inductance can be obtained: $L = 35.6\,\text{nH}$.

The fabricated ESS antenna and its measurement setup are shown in Figure 5.

Figure 6 presents the comparison of measured, simulated and equivalent circuit model results. From Figure 6, we can see that the antenna does not match $50\,\Omega$ in the working UHF band (865–

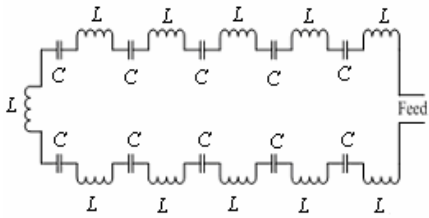

Figure 4. Equivalent circuit model of Figure 2(a).

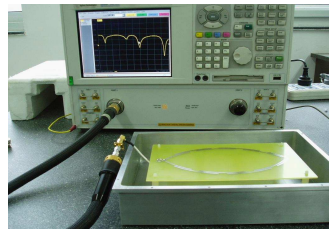

Figure 5. Fabricated ESS RFID reader antenna structure and measurement.

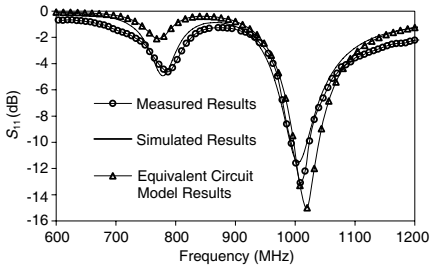

Figure 6. Comparison of S parameters for the fabricated antenna shown in Figure 5.

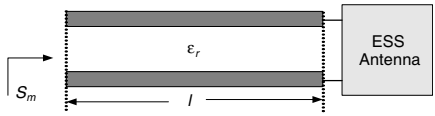

Figure 7. The cascaded model of the measurement method shown in Figure 5.

868 MHz), and there is clear difference in the return loss between the simulated (−0.8 dB) and measured (−1.3 dB) results, which will result in a discrepancy in simulated and measured input impedance. In order to match 50 Ω, a matching network is required to design based on the measured input impedance instead of simulated one. Then obtaining the accurate input impedance is the key step for the accurate matching network design.

Figure 7 shows the cascaded model of Figure 5, where the coaxial line was modeled by transmission line with length l (l = 140 mm). Based on the above measurement method in Figure 5, we obtain the S parameter S_m of both the antenna and the coaxial line. By using de-embedding technology, the effect of the coaxial line can be removed and the antenna S parameter can be obtained as [8, 9],

$$S_{Ant} = S_m e^{j2\beta l} = R_e(S_{Ant}) + jI_m(S_{Ant}) \tag{3}$$

where S_{Ant} is the antenna S parameter, and β is phase constant. Figure 4 shows the results in the form of sum of real and imaginary parts, and $\mathrm{Re}\,(S_{Ant})$ and $\mathrm{Im}\,(S_{Ant})$ represent the real and imaginary part of S_{Ant}, respectively.

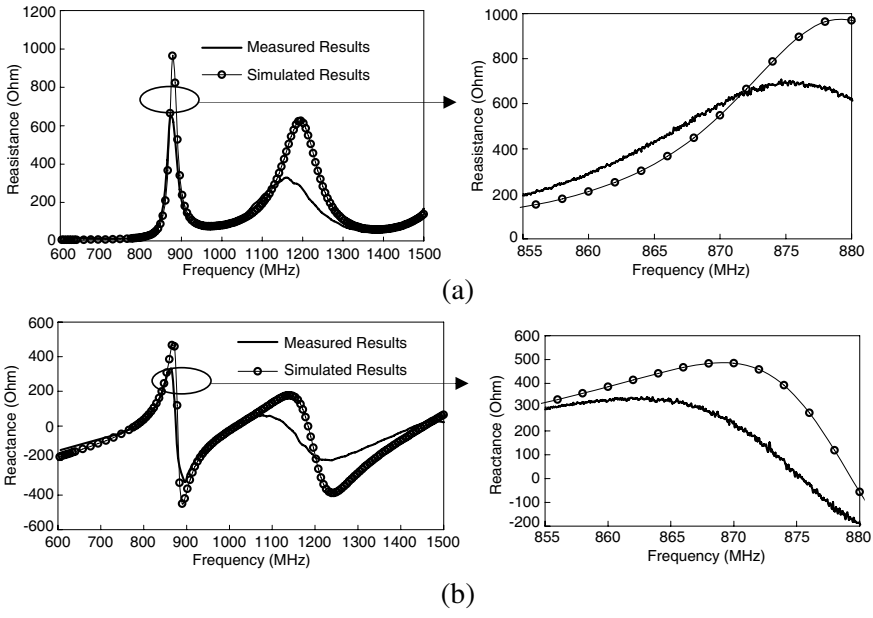

Figure 8. Comparison of impedance between the simulated and measured results after de-embedding. (a) Resistance. (b) Reactance.

Then the real and imaginary parts of the antenna input impedance can be obtained as follows.

$$R_e(Z_{Ant}) = \frac{Z_0 \cdot \left[1 - R_e^2(S_{Ant}) - I_m^2(S_{Ant})\right]}{\left[1 - R_e(S_{Ant})\right]^2 + I_m^2(S_{Ant})} \quad (4)$$

$$I_m(Z_{Ant}) = \frac{2Z_0 \cdot I_m(S_{Ant})}{\left[1 - R_e(S_{Ant})\right]^2 + I_m^2(S_{Ant})} \quad (5)$$

where Z_0 is the characteristic impedance of the coaxial line.

Figures 8(a) and (b) show the real and imaginary parts of the measured impedance for the ESS antenna in Figure 2(a). From Figure 8, we obtain the measured input impedance of the antenna at 866 MHz is $Z_{Ant\_M} = 462 + j316\,\Omega$, while the simulated input impedance is $Z_{Ant\_S} = 366 + j467\,\Omega$.

4. ANTENNA MATCHING NETWORK

Based on the measured input impedance $Z_{Ant\_M} = 462 + j316\,\Omega$ at 866 MHz, the matching network is designed and shown in Figure 9. We can see that the matching network is a balanced circuit. The

Table 2. Values of the lumped elements in the matching network.

Lumped Elements	value
L (nH)	22
$C1$ (pF)	3.3
$C2$ (pF)	3.3
$C3$ (pF)	5.1

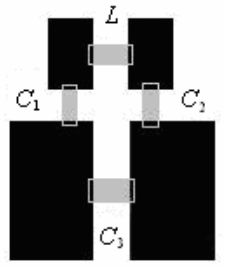

Figure 9. Matching network designed for ESS antenna.

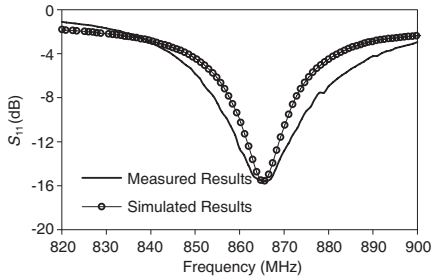

Figure 10. Comparison of measured and simulated results of the ESS antenna after matching.

values of the lumped elements in the matching network are shown in Table 2.

After connecting the matching network, the measured results for the antenna are shown in Figure 10. We can see that the bandwidth is around 11 MHz (860–871 MHz) under the condition of VSWR less than 2, which agrees well with the simulated results.

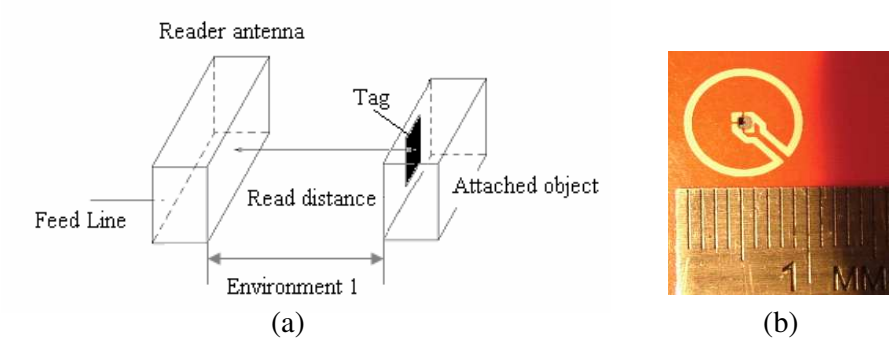

Figure 11. Antenna setup. (a) Test scene of the read distance measurement. (b) The Impinj UHF button near-field tag.

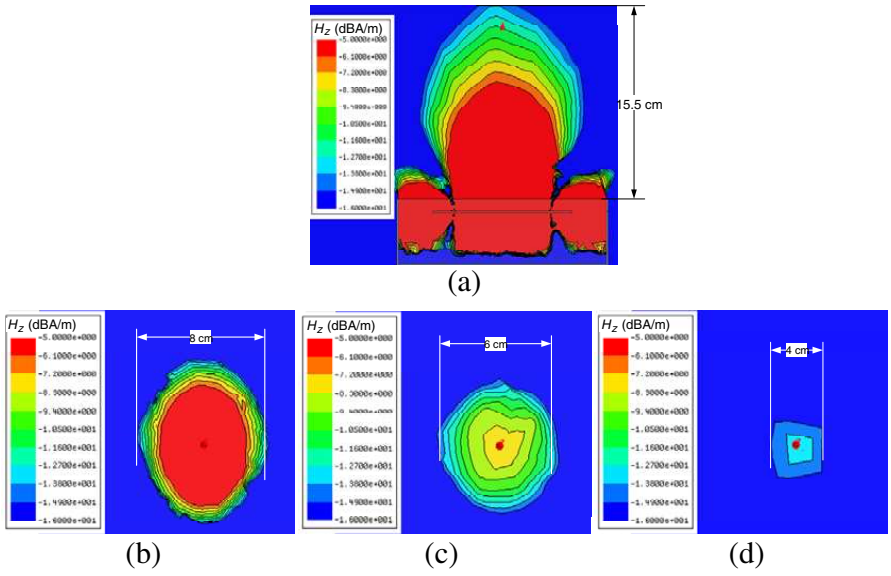

Figure 12. Simulated results of z direction of magnetic field distribution. (a) XOZ plane. (b) $z = 5$ cm at XOY plane. (c) $z = 10$ cm at XOY plane. (d) $z = 15$ cm at XOY plane.

5. THE NEAR-FIELD AND FAR-FIELD PERFORMANCE OF THE ESS NEAR-FIELD ANTENNA

With an Impinj reader and a near-field UHF RFID tag, the reader distance measurement is setup in Figure 11.

Both the environment 1 and the attached object in Figure 11 are considered as air, Figure 12 shows the magnetic field distribution of the ESS antenna at different plane. The simulated results show that the read distance can reach 15.5 cm at XOZ plane, and the read width at XOY plane is 8 cm, 6 cm and 4 cm at $z = 5$ cm, $z = 10$ cm, and $z = 15$ cm, respectively.

The Impinj UHF button near-field tag shown in Figure 11(b) is taken as operating tag. A maximum distance 16.1 cm can be obtained, which agrees well with the simulated results. The measured read width is shown in Figure 13 where the read width at XOY plane is 8 cm, 6 cm and 4 cm at $z = 5$ cm, $z = 10$ cm, and $z = 15$ cm, which agree well with the simulated results.

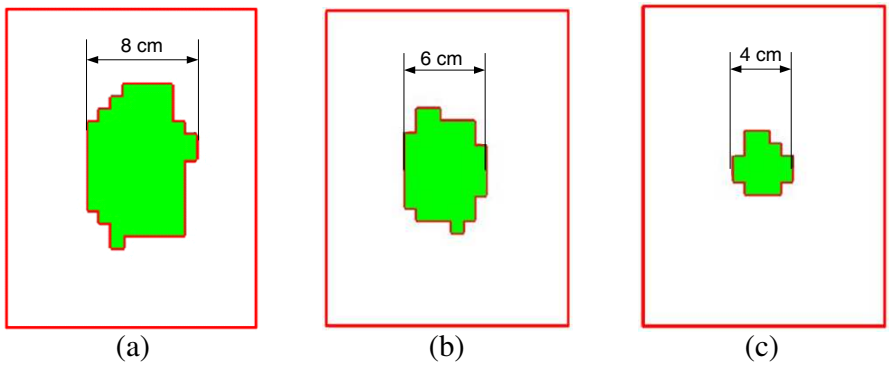

Figure 13. Measured results of read width. (a) $z = 5$ cm at XOY plane. (b) $z = 10$ cm at XOY plane. (c) $z = 15$ cm at XOY plane.

Furthermore, the read distance is also measured under the condition of in or close to aqueous fluids environment. Table 3 compared the measured results for different environment.

From Table 3, we can see that the reading distance shows 15/15.5 cm when the tag is attached to the water-containing items.

Besides, the antenna's radiation pattern was measured in microwave chamber. Figure 14 shows the measured antenna gain at XOZ and YOZ plane, respectively. We can see that the far-field gain achieves 7 dBi at 866 MHz, and the beamwidth is less than 100 degree.

Table 3. Comparison of measured and simulated read distance.

Environment Setup Environment 1/Attached object	Measured Results
air/air	16.1 cm
air/water	15 cm
water/air	15 cm
water/water	15.5 cm

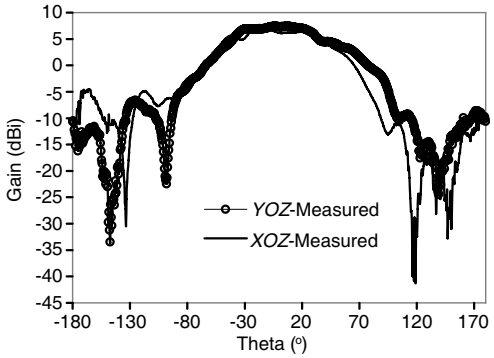

Figure 14. Measured radiation pattern and gain at 866 MHz.

6. CONCLUSION

An eye-shaped segmented near-field UHF RFID reader antenna is proposed to satisfy the required read width and read distance. The key consideration is to keep the current along the eye-shaped loop in equal magnitude and in phase. The proposed antenna has demonstrated the capability of producing a strong magnetic field distribution for special read width and distance requirement. Such a design is suitable for special UHF near-field RFID reader application.

ACKNOWLEDGMENT

This work was supported in part by National High Technology Research Plan of China (863)2009ZX03007-003; Siemens LTD., China, and Program for new Century Excellent Talents 2007 (NECT-07-0108). The Authors thank Prof. Ling Wang and Prof. Changying Wu for their help on antenna gain measurement.

REFERENCES

1. Finkenzeller, K., *RFID Handbook*, 2nd edition, Willey & Sons, New York, 2004.
2. "UHF Gen 2 for item-level tagging," available at http://www.impinj.com/files/MR_GP_ED_00003_ILT.pdf.
3. "Item-level visibility in the pharmaceutical supply chain: A comparison of HF and UHF RFID technologies," available at http://www.tagsysrfid.com/content/download/290/2166/version/1/file/TAGSYS-TI-Philips-White-Paper.pdf.
4. Tan, M., Y. Liu, J. Zeng, X. Li, et al., *RFID Systems Technology and Application Guide*, China Machine Press, Beijing, Apr. 2007.
5. Dobkin, D. M., "Segmented magnetic antennas for near-field UHF RFID," *Microwave Journal*, Vol. 50, No. 6, Jun. 2007.
6. Li, X., J. Liao, Y. Yuan, and D. Yu, "Segmented coupling eye-shape UHF band near field antenna design," *APMC 2009*, 2401–2404, Singapore, #1394, 2009.
7. Qian, X., C. K. Goh, and Z.-N. Chen, "Segmented loop antenna for UHF near-field RFID applications," *Electro. Lett.*, Vol. 45, No. 17, 872–873, Aug. 2009.
8. Li, X. and J. Gao, *MW/RF Measurement Foundation*, China Machine Press, Beijing, Jun. 2007.
9. Liao, J. and X. Li, "A low-cost impedance measurement method for UHF band RFID near field antenna," *IEEE ICCTA 2009*, 32–35, Beijing, 2009.
10. Xu, Z. and X. Li, "Aperture coupling two-layered dual-band RFID reader antenna design," *IEEE International Conference on Microwave and Millimeter Wave Technology*, Apr. 2008.
11. Fan, Z., S. Qiao, H.-F. Jiang Tao, and L.-X. Ran, "A miniaturized printed dipole antenna with V-shaped ground for 2.45 GHz RFID readers," *Progress In Electromagnetics Research*, Vol. 71, 149–158, 2007.
12. Evizal, T. B. A. Rahman, S. K. B. A. Rahim, and M. F. Jamlos, "A multi band mini printed omni directional antenna with V-shaped for RFID applications," *Progress In Electromagnetics Research B*, Vol. 27, 385–399, 2011.
13. Lazaro, A., D. Girbau, and R. Villarino, "Effects of interferences in UHF RFID systems," *Progress In Electromagnetics Research*, Vol. 98, 425–443, 2009.
14. Mahmoud, K. R., "Design optimization of a bow-tie antenna for 2.45 GHz RFID readers using a hybrid Bso-Nm algorithm,"

Progress In Electromagnetics Research, Vol. 100, 105–117, 2010.

15. Chen, X., G. Fu, S.-X. Gong, J. Chen, and X. Li, "A novel double-layer microstrip antenna array for UHF band RFID," *Journal of Electromagnetic Waves and Applications*, Vol. 23, No. 11–12, 1479–1487, 2009.
16. Razalli, M. S., M. A. Mahdi, A. Ismail, S. M. Shafie, and H. Adam, "Design and development of wireless communication transceiver to support RFID reader at UHF RFID," *Journal of Electromagnetic Waves and Applications*, Vol. 24, No. 14–15, 2063–2075, 2010.
17. Liao, W.-J., S.-H. Chang, Y.-C. Chu, and W.-S. Jhong, "A beam scanning phase array for UHF RFID readers with circularly polarized patches," *Journal of Electromagnetic Waves and Applications*, Vol. 24, No. 17–18, 2383–2395, 2010.